

The 9th Asia-Oceania Symposium on Fire Science and Technology

Numerical studies on the interaction of sprinkler and smoke layer

Cunfeng Zhang^{a,c}, Wanki Chow^{b,*}

^aSchool of Urban Construction and Safety Engineering, Nanjing University of Technology, Nanjing, Jiangsu, China

^bResearch Centre for Fire Engineering, The Hong Kong Polytechnic University, Hong Kong, China

^cState Key Laboratory of Fire Science, University of Science and Technology of China, Hefei, Anhui, China

Abstract

Sprinklers are the most reliable method available for controlling building fires. Due to the cooling effect by water spray and drag force produced by the water droplets, sprinkler spray can lead to the loss of stability of the stratified smoke layer. In this paper, the cooling effect of water spray is studied. The smoke layer stability and the mass flow rate are also studied. The Fire Dynamics Simulator (FDS) code, based on the concept of large eddy simulation, is adopted in the present simulation. It has been found that the temperature decrease was almost linear to the working pressure of the sprinkler system. The dimensionless pressure to the smoke penetration depth can be expressed as power function. The spray has great effect on the smoke movement inside the compartment.

© 2013 International Association for Fire Safety Science. Published by Elsevier Ltd. Open access under [CC BY-NC-ND license](http://creativecommons.org/licenses/by-nc-nd/4.0/). Selection and peer-review under responsibility of the Asian-Oceania Association of Fire Science and Technology

Keywords: Sprinkler; Stability; Mass flow; Drag force; Cooling

Nomenclature

A	surface area (m ²)	\dot{m}_b'''	mass loss/production rate per unit volume (kg/m ³)
c	specific heat (J/kg K)	p	Pressure (N/m ²)
C_D	drag coefficient	p_d	sprinkler working pressure (N/m ²)
C_s	Smagorinsky constant	\hat{P}_d	dimensionless pressure (N/m ²)
C_{sp}	sprinkler proportionality constant	\vec{q}''	total heat flux (convective and radiant) (W/m ²)
d	droplet diameter (μm)	\vec{q}_r''	radiant heat flux (W/m ²)
d_m	volume median droplet diameter (μm)	\dot{q}_c'''	heat release rate per unit volume (W/m ³)
d_n	sprinkler orifice diameter (m)	\dot{q}_d'''	heat absorption rate by droplets per unit volume (W/m ³)
D_i	diffusion coefficient for species i (m ² /s)	S	penetration depth (m)
\vec{f}_D	drag force (N)	\hat{S}_{ij}	strain rate tensor
\vec{g}	gravity vector (m/s ²)	\hat{S}	dimensionless smoke penetration depth
h	convective heat transfer coefficient (W/m ² K); smoke layer thickness (m)	t	Time (s)
h_i	enthalpy for species i (J)	\vec{u}	Velocity (m/s)
h_m	mass transfer coefficient	u_{sp}	droplet velocity at sprinkler orifice (m/s)
h_s	enthalpy for smoke (J)	We	Weber number

* Corresponding author: Tel: +852 2766 5843; Fax: +852 2765 7198.
E-mail address: bewkchow@polyu.edu.hk.

h_v	heat of evaporation (kJ/kg)	Y	mass fraction
k	thermal conductivity (W/ m K)	Y_s	water vapor mass fraction at saturation conditions
m	Mass, mass flow rate (kg, kg/s)		
<i>Greek Symbols</i>			
ε	turbulence energy dissipation rate (J/ kg s)	σ_d	surface tension of water (N/m)
Δ	grid cell length (m)	$\tau_{i,j}$	stress tensor
ρ	Density (kg/m ³)	μ	dynamic viscosity (N s/m ²)
σ	log-normal distribution coefficient	γ	Rosin-Rammler distribution exponent
<i>Subscripts</i>			
d	droplet	i,j	$i^{\text{th}}, j^{\text{th}}$ species; tensor components
D	drag	s	smoke

1. Introduction

It is required by the fire regulations of China mainland to install automatic sprinkler systems in buildings such as hotels, factories and shopping malls. However, due to the cooling effect by the water spray, the buoyancy of the hot smoke layer, which supports the stratification, would decrease. On the other hand, the drag force produced by the water droplets would also drag the smoke downward. These two factors both can lead to the loss of stability of the stratified smoke layer. The smoke would fall down to the floor, which is call “smoke logging”. It is a risk to the smoke ventilation and human evacuation during a fire [1-11]. Therefore, it is essential to carefully study the interaction of a smoke layer with a sprinkler.

The problem on the stability of smoke layer under water spray was first discussed by Bullen [1]. The smoke layer was considered as a constant thickness. The sprinkler spray was taken as spherical droplets with constant diameter calculated by the sprinkler pressure. A physical parameter known as the drag-to-buoyancy ratio for the entire smoke layer was taken as the criterion for its stability. Morgan and Baines further developed the model by including the convective heat transfer between the sprinkler spray and fire smoke [2-3]. A distribution function of sprinkler droplets was also included by Morgan [2]. In Cooper’s model, it was considered that the smoke layer element of unit volume below the sprinkler nozzle was pulled down by the drag force of sprinkler droplets and pushed up by its own buoyancy [4]. Due to the cooling effect and drag force of water spray, the venting system would not be so effective [5-7]. The smoke behaviour in the compartment would also be affected. Due to the drag force of water droplets, the mass flow pattern would change [8].

There are many numerical simulations on the fire smoke and spray. However, these simulations are mainly studied on the interaction of fire plume and the spray [9-12]. The stability of smoke is seldom studied in the numerical simulation. There are also some experiments on the interaction of spray and smoke [12-17]. Due to the cost of experiments, few experiments could be done. To study the phenomena on the spray and fire smoke, CFD model is a good choice [18]. In this paper, the cooling effect is studied. The smoke layer stability and the mass flow rate are also studied. The Fire Dynamics Simulator (FDS) code, based on the concept of large eddy simulation, is adopted in the present simulation.

2. Mathematical model and parameters

Fire Dynamics Simulator version 5.5.3 (FDS) which is developed by NIST was used here for the numerical simulation [19]. The model solves numerically a form of the Navier-Stokes equations appropriate for low-speed, thermally-driven flow with an emphasis on smoke and heat transport from fires. The core algorithm is an explicit predictor-corrector scheme that is second order accurate in space and time. Turbulence is treated by means of the Smagorinsky form of Large Eddy Simulation (LES). Lagrangian particles are used to simulate smoke movement, sprinkler discharge, and fuel sprays. The model has been successfully tested for a range of fire-related problems, most extensively for natural convective flows and smoke movement [20, 21].

The grids used in computations would have a major impact on the simulation results. In order to select an appropriate cell size, four grids (30 cm, 20 cm, 10 cm and 7.7 cm) were tried in the computations. The results from 30 cm cell size have the largest deviations in these computations. At the fire plume area, the results from 20 cm cells and 10 cm cells are close to each other. For the places just under the sprinkler head, the results are almost same except the 30 cm cells. However, for the place near the door, the results calculated by 10 cm and 7.7 cm cells are close. So the 10cm cells were used in this paper. The same cells were also chosen by Novozhilov in the simulation of sprinkler interaction with a fire ceiling jet [18].

2.1. Model description

The following is the summary of the model [19].The flow and energy equations (for ideal gas) are considered in a weakly-compressible approximation:

$$\frac{\partial \rho}{\partial t} + \nabla \cdot (\rho \bar{u}) = \dot{m}_b''' \tag{1}$$

$$\frac{\partial}{\partial t}(\rho \bar{u}) + \nabla \cdot (\rho \bar{u} \otimes \bar{u}) + \nabla p = \rho \bar{g} + \bar{f}_D + \nabla \cdot \tau_{i,j} \tag{2}$$

$$\frac{\partial}{\partial t}(\rho h_s) + \nabla \cdot (\rho h_s \bar{u}) = \frac{Dp}{Dt} + \dot{q}_c''' - \dot{q}_d''' - \nabla \cdot \bar{q}'' + \tau_{i,j} \cdot \nabla \bar{u} \tag{3}$$

The term \bar{q}'' represents the total conductive and radiant heat fluxes:

$$\bar{q}'' = -k \cdot \nabla T - \sum_i h_i \rho D_i \nabla Y_i + \bar{q}_r'' \tag{4}$$

There is a term in the energy equation known as the dissipation rate, ε , the rate at which kinetic energy is converted to thermal energy by viscosity:

$$\varepsilon \equiv \tau_{ij} \cdot \nabla \bar{u} = \mu \left(2 \hat{S}_{ij} \cdot \hat{S}_{ij} - \frac{2}{3} (\nabla \bar{u})^2 \right) \tag{5}$$

Following the analysis of Smagorinsky [22], the viscosity μ is modeled:

$$\mu \equiv \mu_{LES} = \rho (C_s \Delta)^2 \left(2 \hat{S}_{ij} \cdot \hat{S}_{ij} - \frac{2}{3} (\nabla \bar{u})^2 \right)^{1/2} \tag{6}$$

where C_s is an empirical constant and Δ is a length on the order of the size of a grid cell. The bar above the various quantities denotes that these are the resolved values, meaning that they are computed from the numerical solution sampled on a grid.

Water spray is represented by an ensemble of Lagrangian particles. The force term \bar{f}_D represents the momentum transferred from the droplets to the gas. It is obtained by summing the force transferred from each droplet in a grid cell and dividing by the cell volume

$$\bar{f}_D = \frac{1}{8} \frac{\sum \rho C_D \pi d^2 |\bar{u}_d - \bar{u}| (\bar{u}_d - \bar{u})}{\delta x \delta y \delta z} \tag{7}$$

where C_D is the drag coefficient, $\delta x \delta y \delta z$ is the volume of the grid cell. The momentum, mass, and energy balances for each droplet are governed by

$$\frac{d}{dt}(m_d \bar{u}_d) = -\pi \frac{d^2}{8} \rho C_D |\bar{u}_d - \bar{u}| (\bar{u}_d - \bar{u}) + m_d \bar{g} \tag{8}$$

$$\frac{dm_d}{dt} = -A_d h_m (Y_s - Y_g) \tag{9}$$

$$m_d c_d \frac{dT_d}{dt} = A_d h (T_g - T_d) + \frac{dm_d}{dt} \cdot h_v \tag{10}$$

Here, the vapor mass fraction of the gas, Y_g , is obtained from the gas phase mass conservation equations, and the liquid equilibrium vapor mass fraction, Y_s , is established from the Clausius-Clapeyron equation.

The most important parameter of the model is the sprinkler spray patterns. The size distribution is expressed in terms of its Cumulative Volume Fraction (CVF). The CVF for a sprinkler can be well presented by a combination of log-normal and Rosin-Rammler distributions [19]

$$F(d) = \begin{cases} \frac{1}{2\pi} \int_0^d \frac{1}{\sigma d'} e^{-\frac{[\ln(d'/d_m)]^2}{2\sigma^2}} dd' & (d \leq d_m) \\ 1 - e^{-0.693(\frac{d}{d_m})^\gamma} & (d_m < d) \end{cases} \quad (11)$$

where γ and σ are empirical constants equal to about 2.4 and 0.6 respectively. The median droplet diameter, d_m , was estimated using the formula reported by You [23]:

$$d_m = \frac{C_{sp} d_n}{W_e^{1/3}} \quad (12)$$

$$W_e = \frac{\rho_a u_{sp}^2 d_n}{\sigma_d} \quad (13)$$

where C_{sp} is the sprinkler constant. For the orifice diameters of 16.3 mm, 13.5 mm, 12.7 mm, the constants were approximately 4.3, 2.9 and 2.3, respectively.

The above descriptions are just the outlines of the FDS model. The details on this model can refer to the Fire Dynamics Simulator (Version 5), Technical Reference Guide [15].

2.2. Model parameters

The schematic diagram of the computational domain is shown in Fig. 1. The dimensions of this domain are 12 m (Length) × 6 m (Width) × 5 m (Height) with openings at both ends. At the end near the fire, the opening is 2 m (width) × 2 m (Height). The air was supplied from this open by natural convection. At the other end, the opening is 2 m (width) × 4 m (Height) for natural smoke ventilation. For the simplicity of calculation, the domain surface is set to be adiabatic.

The 1 m × 1 m rectangular constant fire located at the floor (location F0) was basically modeled as the ejection of gaseous fuel from a solid surface. Two heat release rates were used: 1.0 MW and 1.5 MW. All of the surfaces in the domain were set as non-reacting solid boundary. The initial temperature of walls and ambient air were set to 20 °C.

Table 1. Sprinkler parameters for simulated pressure

Parameter	Values				
Pressure / Bar	0.5	0.75	1.0	1.25	1.5
Flow rate / L/min	56.57	69.28	80.0	89.44	97.98
Droplet volume median diameter / μm	1043.22	911.33	828	768.65	723.32
Droplet initial velocity / m/s	3.95	4.83	5.58	6.24	6.8

Upright sprinkler heads with a 12.7 mm orifice diameter (K factor equals to 80 L/(min bar^{1/2})) were placed 0.1 m apart from the ceiling (Location S0) in the simulation. The spray angles range from 30° to 80° as shown in Fig. 2. The atomization length of water spray is set to 0.2 m. For the working pressure of 1 bar, the median droplet diameter, d_m , equals to 828 μm and the initial droplet velocity, v , is 5.58 m/s. For the other working pressure, the d_m and v can be calculated by the following [18]:

$$d_m(p_d) = 828 \left(\frac{1}{p_d} \right)^{1/3} (\mu m) \quad (14)$$

$$v(p_d) = 5.58\sqrt{p_d} \text{ (m/s)} \tag{15}$$

Table 1 shows the information of sprinkler head. A more details on the sprinkler parameters can be found in reference [18]. The p_d is the sprinkler working pressure in unit of bar. A summary of the sprinkler parameters are list in Table 1. It should be noted that the described parameters are used as the “base” case, and variations of these are performed to quantify sensitivity of the model.

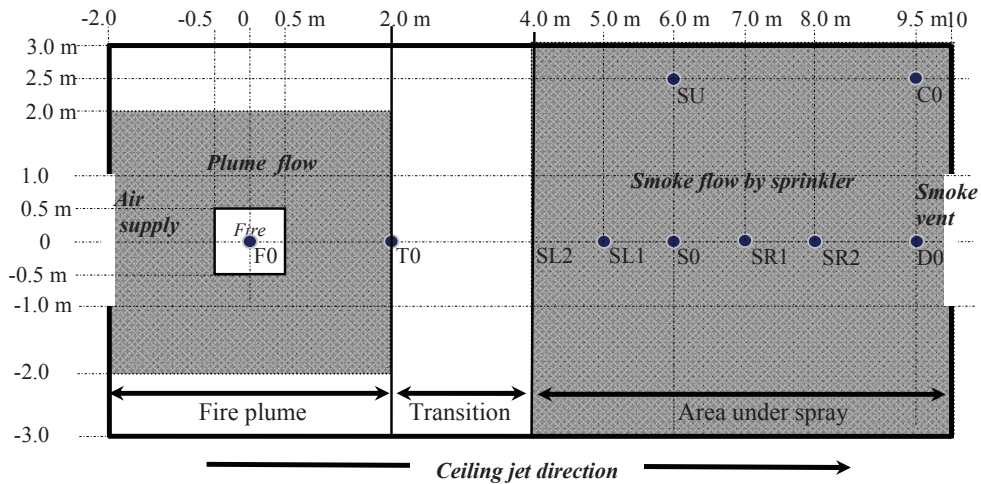


Fig. 1 (a). Simulation domain layout and locations of thermocouple trees.

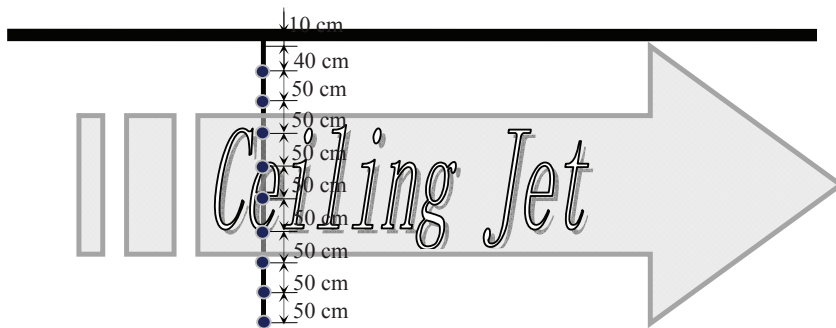


Fig. 1 (b). Details of thermocouple tree.

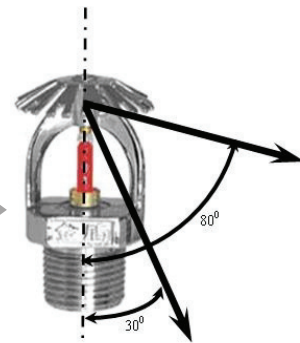


Fig. 2. Definition of spray angles.

The thermocouple trees at the locations marked ● were used to record temperatures of smoke, as shown in Fig. 1(a). These trees are placed 10 cm below the ceiling. As shown in Fig. 1(b), the space of thermocouples in every tree is 50 cm with the exception of the two thermocouples near the ceiling. They are 40 cm apart from each other.

The mass flows at the two openings were recorded. For the air supply opening, the net mass flow (m_{a1}) was calculated. For the ventilation opening, the total mass flows in (m_{a2}) and out (m_D) of the opening were simulated. The mass flows across two planar areas, marked gray in Fig. 1(a), at the height of 3m from the floor were also calculated. The net mass flow across the left area in Fig. 1 (a) (4 m × 4 m) is considered as fire plume mass flow (m_p). The area just under the sprinkler head is 6 m × 6 m. The mass flows up (m_u) and down (m_E) the area are both recorded.

3. Results and discussion

A total of 10 cases were simulated using FDS. There are grouped into two sets due to different heat release rate of fire: 1 MW and 1.5 MW. Sprinkler head was set on after the fire started 90 seconds. The working pressure of sprinker head varied from 0.5 bar to 1.5 bar. Typical results of smoke development are shown in Figs. 3-5.

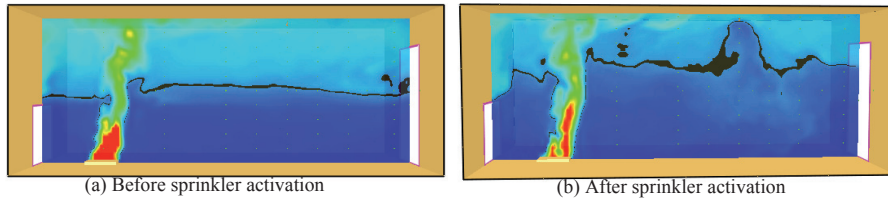


Fig. 3. Slice of smoke temperature at different conditions.

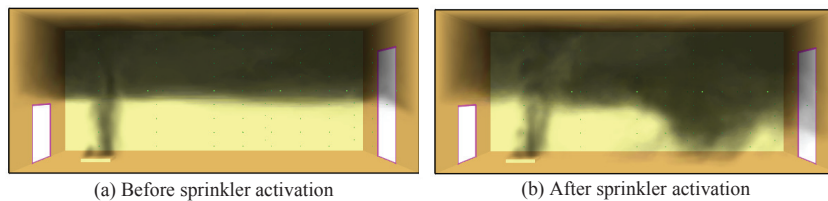


Fig. 4. Smoke view at different conditions.

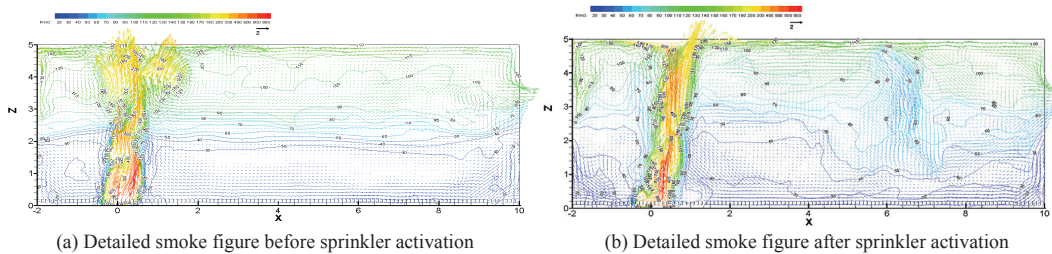


Fig. 5. Temperature distribution and velocity vectors.

At about 30 s after the fire ignition, a steady smoke layer was formed and the hot smoke flowed out across the upper part of the smoke vent (Figs. 3(a) and 4 (a)). A more detailed figure on temperature distribution and velocity vector was shown in Fig. 5 (a). The contour lines are parallel and nearly horizontal. There was a clear smoke-air interface at about 2 m above the floor. From the ceiling to smoke-air interface, the temperature declined smoothly. The velocity vector in Fig. 5 is the smoke velocity projected at the central plan of $y = 0$. It can be seen from the figure that the downward velocity of smoke was at about 0.5~1.0 m/s when the sprinkler head was not activated. Due to the high temperature of hot smoke, the out flow velocity was greater than 3 m/s, much higher than the downward smoke.

There are great differences when the sprinkler was activated. Due to the cooling effect and the drag force on the smoke, the temperature would decrease apparently. The smoke would not keep on the ceiling and move downward. In some situations, the smoke would not keep layer and the smoke logging [1] would happened. Whether or not the smoke logging happened was decided by the smoke temperature and the spray parameters. The results shown in Figs. 3(b)-5(b) came from the case A3. The smoke temperature contour was convex towards the sprinkler head. Comparing with the condition before sprinkler activation, the smoke temperature after sprinkler activation at the same height was low. The downward velocity under sprinkler spray increased to larger than 2 m/s. The out flow velocity did not vary apparently.

Table 2. Temperature of smoke layer

Case NO.	HRR/MW	Sprinkler Pressure/bar	Temperature / °C		Smoke layer thickness/mm	penetration depth/mm
			Smoke layer	Under sprinkler head		
0	1.0	0	103.9	103.8	2000	0
A1	1.0	0.5	93.1	71.9	2000	670
A2	1.0	0.75	88.6	64.8	2000	950
A3	1.0	1.0	85.2	60.0	2000	1120
A4	1.0	1.25	81.2	55.9	2000	1580
A5	1.0	1.5	78.8	53.2	2000	1800*
B0	1.5	0	132.4	132.5	2200	0
B1	1.5	0.5	118.0	93.3	2200	550
B2	1.5	0.75	112.8	81.9	2200	780
B3	1.5	1.0	109.0	76.7	2200	900
B4	1.5	1.25	107.5	72.2	2200	1300
B5	1.5	1.5	101.5	66.7	2200	1700

*: The smoke descended to the floor.

3.1. Cooling effect

For the convenience of discussion, the domain is divided into three parts according to the horizontal distance to the sprinkler head: fire plume part, the area under the water spray and the transition region between them (as shown in Fig. 1). In this part, only the area under the water spray would be discussed.

According to the fire regulations of China mainland, the protection area of a sprinkler head could not be larger than 20 m² and the distance between sprinkler heads must be less than 4.5 m. The radius of water-wetted area is about 3 m for the 5 m high building. The thermocouple trees S0, SL1, SL2, SR1, SR2 and SU are used to simulate the temperature change of smoke under the sprinkler.

The temperatures of smoke layer under the water spray were listed in Table 2. These values were calculated by SL1, SL2, SR1, SR2 and SU. The thermocouples of these trees in the smoke layer were used for average calculation. Case A0 and B0 were the values before the sprinkler head was activated. The higher the working pressure was, the lower temperature the smoke had. The temperature decrease was almost linear to the working pressure (Fig. 6).

3.2. Stability of smoke layer

Due to the drag force of water spray, once the sprinkler was activated, the smoke would descend. The smoke-air interface surface would not keep horizontal. The smoke penetration depth was decided by the fire heat release rate and the working pressure of water spray. When the sprinkler pressure is low, the smoke layer is still stable. The results for the penetration depth were listed in Table 2. The smoke layer thickness in Table 2 was the thickness before the sprinkler head was activated. The penetration depth was decided by the temperature contour lines and the smoke view after sprinkler activation. For the smoke layer thickness calculation, N-percent method was used. For the penetration depth, just a simple temperature threshold, 40 °C~45 °C, was used. The smoke view was also used for reference to aid the decision of depth.

For quantitative description of relationship on the smoke penetration depth and the working pressure and heat release rate of the fire, dimensionless pressure (\hat{P}_d) and smoke penetration depth (\hat{S}) are defined as followed:

$$\begin{aligned}\hat{P}_d &= P_d / \rho_d V_0^2 \\ \hat{S} &= S / h\end{aligned}\quad (16)$$

The reference velocity, V_0 , is defined as [17, 24]:

$$V_0 = \left(\frac{g \dot{Q}}{\rho_0 c_p T_0 H} \right)^{1/3} \tag{17}$$

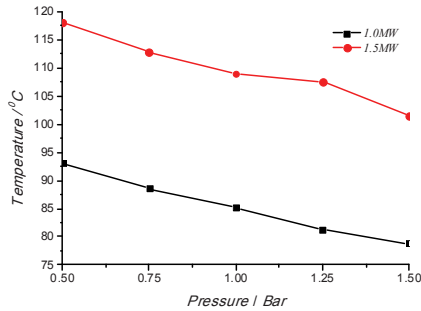


Fig. 6. Smoke layer temperature after sprinkler activation.

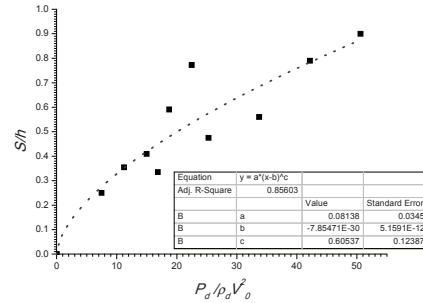


Fig. 7. Relationship between dimensionless thickness and dimensionless pressure.

where H is the height of the computational domain and \dot{Q} is the fire heat release rate. The symbol h is the smoke layer thickness, while S is the smoke penetration depth.

The results of \hat{S} to the dimensionless pressure are plotted in Fig. 7. The dotted line in the figure is the corresponding fitting curve. As the parameter b in the Fig. 7 is very small, the curve and its corresponding correlation coefficient R for each sprinkler type can be expressed approximately as the below:

$$\hat{S} = 0.08138 \hat{P}_d^{0.60537} \tag{18}$$

$$R^2 = 0.85603$$

3.3. Mass flow

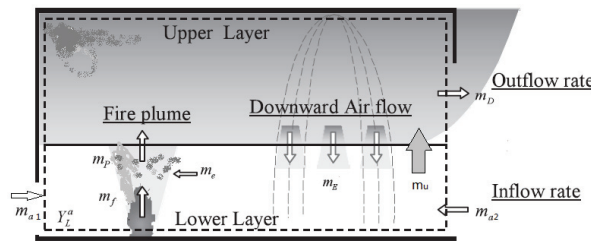


Fig. 8. Conceptual diagram of smoke behaviour

Figure 8 is a conceptual diagram of smoke behavior in the compartment during sprinkler system activation. The fire source and the water application are intentionally separated in order to explain the influence of droplets of water on smoke behavior. It is also assumed that the compartment is in stationary state. The mass conversation could be expressed as:

$$m_p + m_u = m_f + m_{a1} + m_{a2} + m_E$$

$$m_p + m_u = m_D + m_E$$

$$m_p = m_f + m_e$$

$$m_e = m_E + m_{a1} + m_{a2}$$
(19)

Here, the m_p is the mass flow rate of fire plume, the m_u is the mass flow rate into the smoke layer across the interface, the m_f is the mass loss rate of combustion material, the m_{a1} and m_{a2} is the total mass flow rate into the domain by the two opening and the m_D is the total mass flow in the domain by the smoke vent. Because the value of m_f is very small, the burning rate can be ignored. The followed equation can be deduced:

$$m_D = m_{a1} + m_{a2} \tag{20}$$

The simulation results for these mass flows were listed in Table 3. The corresponding figures were shown in Fig. 9. The m_u' and m_E' are the mass flows across the area just under the sprinkler head. It could be seen that the sprinkler had some effects on the mass flow. The downward flow and the plume increased apparently. The upward flow m_u' increased also. The inflow rate m_{a1} , m_{a2} and outflow rate m_D did not change much except for some particular working pressure. For the HRR 1MW, the particular pressure was 1 bar. And for the HRR 1.5 MW, it was 1.25 bar. It can be deduced that the spray has great effect on the smoke movement inside the compartment. However, the inflow and outflow do not change much. The reason is that in the model calculated in this paper, the sprinkler head was placed too far away from the vent. The water droplets can't move to the area near the vent. The smoke flow near the vent is mainly drove by the smoke buoyancy and the pressure difference between the computational domain and the outside.

Because the m_u' and m_E' are the mass flows across the area just under the sprinkler head, substituting these values into the Eq. (19) cannot obtain good results. It means that in the transition area (Fig. 2), the mass flow across the smoke-air interface was significant. The great mass of downward flow forced by sprinkler spray would move back into the smoke layer in the transition area.

Table 3. Mass flow results

Case NO.	HRR/ MW	Sprinkler Pressure/bar	Mass flow/ kg/s					
			m_{a1}	m_{a2}	m_u'	m_D	m_E'	m_p
A0	1.0	0	2.6	2.5	2.4	5.2	4.1	5.6
A1	1.0	0.5	2.6	2.7	3.6	5.3	6.8	6.3
A2	1.0	0.75	2.5	2.6	3.7	5.2	7.3	6.5
A3	1.0	1.0	2.1	2.8	3.9	4.9	7.5	6.1
A4	1.0	1.25	2.3	2.5	3.8	4.9	8.5	7.1
A5	1.0	1.5	2.2	2.5	3.7	4.8	9.1	7.4
B0	1.5	0	3.0	3.0	2.5	6.2	4.6	6.9
B1	1.5	0.5	3.1	3.0	3.6	6.1	7.5	7.6
B2	1.5	0.75	2.9	2.9	3.7	6.0	8.2	7.7
B3	1.5	1.0	2.8	2.9	4.0	5.9	8.7	7.7
B4	1.5	1.25	2.3	3.1	4.2	5.6	8.6	7.0
B5	1.5	1.5	2.8	2.8	4.2	5.8	9.4	8.2

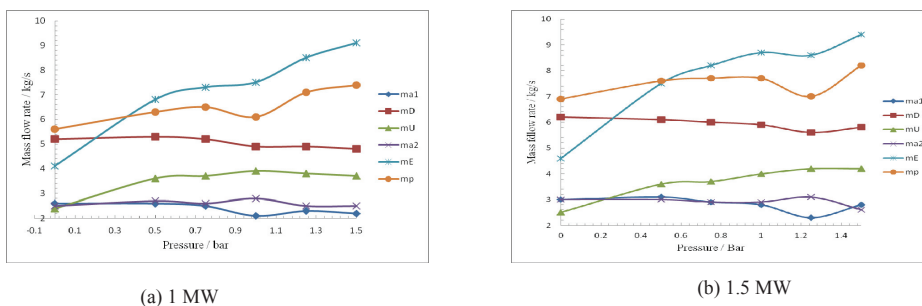


Fig. 9. Mass flow for different pressures.

4. Conclusions

The interaction of fire smoke and the water spray was studied in this paper. Fire Dynamics Simulator version 5.5.3 (FDS) which is developed by NIST was used for the numerical simulation. A total of 10 cases with different sprinklers and different fire heat release rates were calculated. The following observations are made:

Due to the cooling effect, the temperature would decrease apparently once upon the sprinkler was activated. The temperature decrease was almost linear to the working pressure.

Due to the drag force of water spray, once the sprinkler was activated, the smoke would descend. The dimensionless pressure (\hat{P}_d) to the smoke penetration depth (\hat{S}) can be expressed as:

$$\begin{aligned}\hat{S} &= 0.0839\hat{P}_d^{0.596} \\ R^2 &= 0.7477\end{aligned}\quad (21)$$

The spray has great effect on the smoke movement inside the compartment. Because the sprinkler head was placed too far away from the vent, the inflow and outflow do not change much.

Acknowledgements

This work was supported by the Opening Fund of State Key Laboratory of Fire Science under Grant No.HZ2010-KF08 and the Opening Fund of State Key Laboratory of Building Safety and Environment under Grant No.bsbe2010-10.

References

- [1] Bullen, M. L., 1974. The Effect of a Sprinkler on the Stability of a Smoke Layer beneath a Ceiling. Fire Research Note 1016, Fire Research Station, Borehamwood, UK.
- [2] Morgan, H. P., 1979. Heat Transfer from a Buoyant Smoke Layer beneath a Ceiling to a Sprinkler Spray 1-A Tentative Theory, Fire and Materials 3(1), p. 27.
- [3] Morgan, H. P., Baines, K., 1979. Heat Transfer from a Buoyant Smoke Layer beneath a Ceiling to a Sprinkler Spray 2-An Experiment, Fire and Materials 3(1), p. 34.
- [4] Cooper, L. Y., 1995. The Interaction of an Isolated Sprinkler Spray and a Two-Layer Compartment Fire Environment: Phenomena and Model Simulations, Fire Safety Journal 25(2), p. 89.
- [5] McGrattan, K. B., Hamins, A., Stroup, D., 1998. Sprinkler, Smoke and Heat Vent, Draft Curtain Interaction—Large Scale Experiments and Model Development, NISTIR 6196-1. Building and Fire Research Laboratory, National Institute of Standards and Technology, Gaithersburg, MD.
- [6] Beyler, C. L., Cooper, L. Y., 2001. Interaction of Sprinklers with Smoke and Heat Vents, Fire Technology 37(1), p. 9.
- [7] Hsieh, T. L., CHIEN, S. W., Chung, K. C., Lin, C. H., 2002. The Effect of Smoke Vents on the Sprinklers in a Small Compartment, Journal of Applied Fire Science 11(2), p. 91.
- [8] Ota, M., Kuwana, Y., Ohmiya, Y., Matsuyama, K., Yamaguchi, J., 2009. A Study on Smoke Behavior in a Compartment with Sprinkler System Activation—Simple Predictive Method on Mass Flow Rates Based on Experimental Study, Fire Science and Technology 28(3), p. 88.
- [9] Chow, W. K., Fong, N. K., 1993. Application of Field Modeling Technique to Simulate Interaction of Sprinkler and Fire-Induced Smoke Layer, Combustion Science and Technology 89, p. 101.
- [10] Chow, W. K., Cheung, Y. L., 1994. Simulation of Sprinkler-Hot Layer Interaction Using a Field Model, Fire and Materials 18(6), p. 359.
- [11] Soonil, N., 1996. Development of a Computational Model Simulating the Interaction between a Fire Plume and a Sprinkler Spray, Fire Safety Journal 26, p. 1.
- [12] Hua, J. S., Kumar, K., Khoo, B. C., Xue, H., 2001. A Numerical Study of the Interaction of Water Spray with a Fire Plume, Fire Safety Journal 37, p. 631.
- [13] Ingason, H., Olsson, S., 1992. Interaction between Sprinkler and Fire Vents—Full Scale Experiments, Fire Technology SP Report 1992:11, Swedish National Testing and Research Institute, Sweden.
- [14] Chow, W. K., Tong, A. C., 1994. Experimental Studies on Sprinkler Spray-Smoke Layer Interaction, Journal of Applied Fire Science 4, p. 171.
- [15] McGrattan, K. B., Baum, H. R., Rehm, R. G., Hammins, A., Forney, G. P., Floyd J. E., Hostikka, S., Prasad, K., 2002. Fire Dynamics Simulator (Version 3)—Technical reference guide, NISTIR 6783. Building and Fire Research Laboratory, National Institute of Standards and Technology, Gaithersburg, MD.
- [16] Zhang, C. F., Huo R., Li, Y. Z., 2005. “Stability of Smoke Layer under Sprinkler Water Spray,” ASME’s 2005 Summer Heat Transfer Conference, San Francisco, CA.
- [17] Zhang, C. F., Chow, W. K., Huo R., Zhong, W., Li, Y. Z., 2010. Experimental Studies on Stability of Smoke Layer with a Sprinkler Water Spray, Experimental Heat Transfer 23(3), p. 196.
- [18] O’Grady, N., Novozhilov, V., 2009. Large Eddy Simulation of Sprinkler Interaction with a Fire Ceiling Jet, Combustion Science and Technology 181(7), p. 984.
- [19] McGrattan, K. B., Hostikka, S., Floyd J. E., Baum, H. R., Rehm, R. G., Mell, W. E., McDermott., R., 2010. Fire Dynamics Simulator (Version 5), Technical Reference Guide, Volume 1: Mathematical Model. Gaithersburg, Maryland, USA, Oct. 2010.
- [20] Mell, W. E., McGrattan, K. B., Rehm, R. G., 1996. Numerical Simulation of Combustion in Fire Plumes, Proceedings of the Combustion Institute 26 (1), p. 1523.
- [21] Xin, Y., Filatyev, S. A., Biswas, K., Gore, J. P., Rehm, R. G., Baum, H. R., 2008. Fire Dynamics Simulations of a One-meter Diameter Methane Fire, Combustion and Flame 153 (4), p. 499.
- [22] Smagorinsky, J., 1963. General Circulation Experiments with the Primitive Equations. I: The Basic Experiment, Monthly Weather Review 91(3), p. 99.
- [23] You, H. Z., 1986. “Investigation of Spray Patterns of Selected Sprinklers with the FMRC Drop Size Measuring System”, Fire Safety Science - Proceedings of the First International Symposium, International Association for Fire Safety Science, pp. 1165-1176.
- [24] Quintiere, J. G., 1989. Scaling Applications in Fire Research, Fire Safety Journal 15(1), p. 3.